J Fluoresc
DOI 10.1007/s10895-015-1582-5

EDITORIAL

An ICT-Based Hydrogen Sulfide Sensor with Good Water Solubility for Fluorescence Imaging in Living Cells

Qiuyan Xu [1] · Longwei He [1] · Haipeng Wei [1] · Weiying Lin [1,2]

Received: 19 March 2015 / Accepted: 4 May 2015

Introduction

Hydrogen sulfide (H_2S), traditionally considered to be a toxic gas with the typical smell of rotten eggs and an antioxidant or scavenger for reactive oxygen species (ROS) [1], has recently emerged as a member of the endogenous gaseous transmitter family of signaling molecules including nitric oxide (NO) and carbon monoxide (CO) [2–3]. The endogenous H_2S is produced by the enzymes (such as cystathionine β-synthase, cystathionine γ-lyase, and 3-mercaptopyruvate sulphurtransferase) catalysis action of cysteine or cysteine derivatives in mammalian tissues [4–6]. H_2S plays an important physiological role in many biological processes, for instance, ischemia reperfusion injury, vasodilation, apoptosis, insulin signaling, and oxygen sensing [7–11]. However, abnormal levels of H_2S is associated with various diseases, like Alzheimer's disease [12], Down's syndrome [13], diabetes [10], and liver cirrhosis [14]. Therefore, it's very significant for monitoring H_2S using sensitive, selective, and water-soluble fluorescent probe in the native biological environment.

Fluorescence imaging has been widely used as a powerful tool for monitoring biomolecules within the context of living systems with high spatial and temporal resolution [15–16]. Naphthalimide dye is the favorable building block for constructing fluorescent probes because of its excellent photophysical properties, such as high extinction coefficients, excellent quantum yields, and great photostability. In addition, azido group is well-known for sensitively and selectively responding to H_2S, the electron withdrawing azide is very easy reduced by H_2S affording the electron donating amine [17–26]. Thus, in this work, we employed the naphthalimide chromophore as the signal reporter and azido group as the responding site for H_2S to construct a H_2S probe based on internal charge transfer (ICT) process (Scheme 1). In addition, to enhance the water solubility, we introduced a hydrophilic alcoholic group to the naphthalimide core. Prior to react with H_2S, we supposed that probe **Nap-N_3** has negligible fluorescence. However, interaction of naphthalimide azide with H_2S affords 4-amino-1,8-naphthalimide, which would elicit a significant fluorescence enhancement via ICT process caused by the electron donating amine and the electron withdrawing amide. So, probe **Nap-N_3** might be employed as a turn-on fluorescent probe for detecting H_2S.

Experimental

Materials and Instruments

Unless otherwise stated, all reagents were purchased from commercial suppliers and used without further purification. Solvents used were purified by standard methods prior to use. Twice-distilled water was used throughout all experiments; High resolution mass spectrometric (HRMS) analyses were measured on a Finnigan MAT 95 XP spectrometer;

Electronic supplementary material The online version of this article (doi:10.1007/s10895-015-1582-5) contains supplementary material, which is available to authorized users.

✉ Weiying Lin
weiyinglin2013@163.com

[1] State Key Laboratory of Chemo/Biosensing and Chemometrics, College of Chemistry and Chemical Engineering, Hunan University, Changsha, Hunan 410082, China

[2] Institute of Fluorescent Probes for Biological Imaging, School of Chemistry and Chemical Engineering, School of Biological Science and Technology, University of Jinan, Jinan, Shandong 250022, People's Republic of China

Published online: 19 May 2015

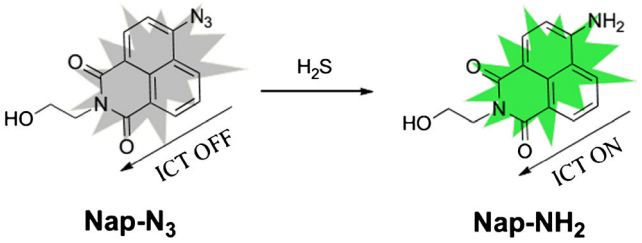

Scheme 1 A turn-on fluorescent H_2S probe based on the proposed ICT switching mechanism

NMR spectra were recorded on an INOVA-400 spectrometer, using TMS as an internal standard; Electronic absorption spectra were obtained on a LabTech UV Power spectrometer; Photoluminescent spectra were recorded with a HITACHI F4600 fluorescence spectrophotometer with a 1 cm standard quartz cell; The fluorescence imaging of cells was performed with OLYMPUS FV1000 (TY1318) confocal microscopy; The pH measurements were carried out on a Mettler-Toledo Delta 320 pH meter; TLC analysis was performed on silica gel plates and column chromatography was conducted over silica gel (mesh 200–300), both of which were obtained from the Qingdao Ocean Chemicals.

Synthesis

The target compound **Nap-N_3** was readily synthesized in just two steps as shown in Scheme 2.

Synthesis of Compound Nap-N_3

The mixture of compounds 4-bromo-1,8-naphthalic anhydride (82.8 mg, 0.3 mmol) and ethanolamine (90 mg, 1.5 mmol) in 5 mL of ethanol was heated at 80 °C under reflux for 4 h. After cooling to room temperature, the reaction solvent was removed under reduced pressure. The resulting residue was a light yellow solid as the crude product of intermediate compound **2**, which was directly carried on the next reaction without further process. The mixture of compound **2** (16 mg, 0.05 mmol) and sodium azide (13 mg, 0.20 mmol) in 3 mL of dry N,N-dimethylformide (DMF) was heated to 90 °C for 3 h in the dark. After cooling to room temperature, the reaction mixture was poured into 100 mL of water and then extracted three times with dichloromethane. The organic phase was collected, washed with brine, and dried with anhydrous $MgSO_4$. The solvent was removed under reduced pressure and the solid residue was purified by flash chromatography column using methanol/dichloromethane (*v*/*v* 1:20) to afford a yellow solid as compound **Nap-N_3** (10 mg, yield 70.9 %). ^{1}H NMR (400 MHz, $CDCl_3$) δ 8.64 (d, J = 7.2 Hz, 1H), 8.58 (d, J = 8.0 Hz, 1H), 8.45 (d, J = 8.4 Hz, 1H), 7.75 (t, J = 7.8 Hz, 1H), 7.47 (d, J = 8.0 Hz, 1H), 4.45 (t, J = 5.2 Hz, 2H), 3.96 (t, J = 5.2 Hz, 2H).^{13}C NMR (100 MHz, $CDCl_3$) δ 164.87, 164.50, 143.84, 132.55, 132.06, 129.13, 126.91, 124.32, 122.29, 118.52, 114.72, 61.85, 42.80. MS (EI) *m*/*z* 282.1 $[M]^+$. HRMS (EI) *m*/*z* calcd for $C_{14}H_{10}N_4O_3$ $[M]^+$: 282.0747. Found 282.0758.

Synthesis of Compound Nap-NH_2

Sodium sulfide (20 mg, 0.25 mmol) was added to the solution of compound **Nap-N_3** (14 mg, 0.05 mmol) in 3 mL DMF/H_2O (*v*/*v* 9:1) mix-solvent. The mixture was stirred for 1.5 h at room temperature in the dark. The reaction mixture was poured into 100 mL of water and then extracted two times with dichloromethane and ethyl acetate (*v*/*v* 5:1). The organic phase was collected, washed with brine, and dried with anhydrous $MgSO_4$. The solvent was removed under reduced pressure and the solid residue was purified by flash chromatography column using methanol/dichloromethane (*v*/*v* 1:10) to afford a yellow solid as compound **Nap-NH_2** (9.5 mg, yield 74.2 %). ^{1}H NMR (400 MHz, DMSO) δ 8.69 (d, J = 8.4 Hz, 1H), 8.42 (d, J = 7.2 Hz, 1H), 8.19 (d, J = 8.4 Hz, 1H), 7.65 (t, J = 8.2 Hz, 1H), 7.56 (s, 2H), 6.89 (d, J = 8.4 Hz, 1H), 4.13 (t, J = 6.6 Hz, 2H), 3.59 (m, 2H).^{13}C NMR (100 MHz, DMSO) δ 164.39, 163.49, 153.23, 134.35, 131.42, 130.18, 129.92, 124.35, 122.23, 119.79, 108.57, 107.91, 58.42, 41.78.MS (EI) *m*/*z* 256.1 $[M]^+$. HRMS (EI) *m*/*z* calcd for $C_{14}H_{12}N_2O_3$ $[M]^+$: 256.0842. Found 256.0844.

Determination of the Fluorescence Quantum Yield

Fluorescence quantum yields for compounds **Nap-N_3** and **Nap-NH_2** were determined by using fluorescein (Φ_f = 0.95

Scheme 2 Synthesis of H_2S sensor Nap-N_3 and the reduced product Nap-NH_2

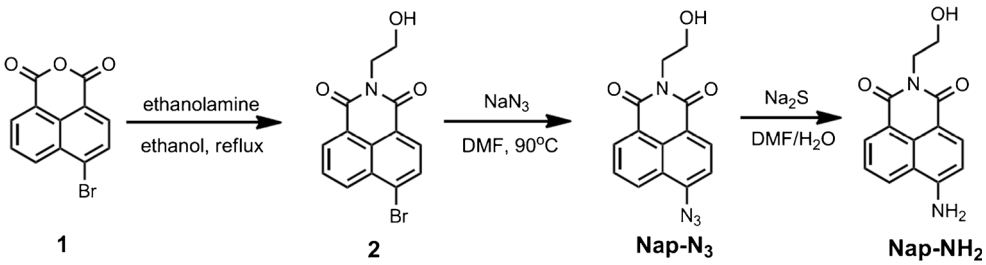

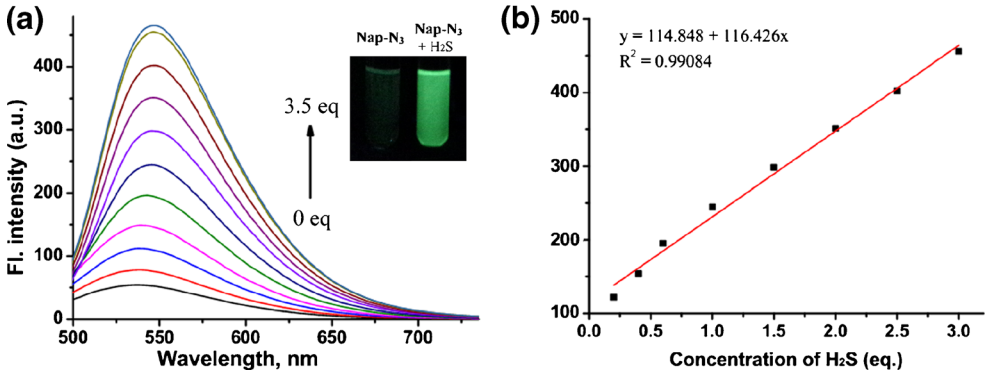

Fig. 1 **a** Fluorescence spectra (λ_{ex} = 408 nm) of 10 μM Nap-N_3 with 0–3.5 eq. of Na_2S in 25 mM phosphate buffer (pH 7.4, containing 2 % ethanol). The inset shows the visual fluorescence color of Nap-N_3 before (*left*) and after (*right*) addition of H_2S (UV lamp, 365 nm). **b** The linear relationship between the fluorescence intensity at 546 nm and the concentration of H_2S

in 0.1 M NaOH aqueous solution) as fluorescence standard [27]. The quantum yields were calculated using the following equation.

$$\Phi_{F(X)} = \Phi_{F(S)}(A_S F_X / A_X F_S)(n_X / n_S)^2$$

Where Φ_F is the fluorescence quantum yield, A is the absorbance at the excitation wavelength, F is the area in the corrected emission spectrum, and n is the refractive index of the solvent used. Subscripts $_S$ and $_X$ refer to the standard and to the unknown, respectively.

HeLa Cells Culture

HeLa cells were cultured in DMEM (Dulbecco's modified Eagle's medium) supplemented with 10 % FBS (fetal bovine serum) in an atmosphere of 5 % CO_2 and 95 % air at 37 °C.

Imaging of Exogenous H_2S in Living Cells

HeLa cells were incubated with 5.0 μM **Nap-N_3** for 20 min in an atmosphere of 5 % CO_2 and 95 % air, and then treated with 20 μM Na_2S for 10 min. Subsequently, the cells were imaged using OLYMPUS FV1000 (TY1318) confocal microscope with an excitation filter of 405 nm and emission channels of 520–570 nm (green channel).

Imaging of Endogenous H_2S in Living Cells

PC-3 cells were incubated with 200 μM cysteine for 60 min in an atmosphere of 5 % CO_2 and 95 % air, and then treated with 5.0 μM **Nap-N_3** for 20 min. Subsequently, the cells were imaged using OLYMPUS FV1000 (TY1318) confocal microscope with an excitation filter of 405 nm and emission channels of 520–560 nm (green channel).

Results and Discussion

Fluorescence Responses to H_2S

With compound **Nap-N_3** in hand, we first evaluated the capability of **Nap-N_3** to detect H_2S in aqueous buffer. The titration of H_2S to the probe **Nap-N_3** (10.0 μM) was performed in 25 mM PBS buffer (pH 7.4) with just 2 % ethanol. As designed, upon excitation at 438 nm, the free sensor displayed faint fluorescence at around 546 nm (Fig. 1a). However, addition of Na_2S (a standard source for hydrogen sulfide) elicited a significant emission enhancement, suggesting that **Nap-N_3** was reduced affording **Nap-NH_2** in the presence of H_2S and ICT process occurred. The fluorescence intensities at 546 exhibited 7.9-fold increase, it's the ICT resonance structure of compound **Nap-NH_2** that contributes mainly to the enhanced fluorescence. The quantum yields of compounds **Nap-N_3** and **Nap-NH_2** were determined 0.0056 and 0.1175, respectively, using a reference fluorescein dye (with a quantum yield of 0.95 in 0.1 M NaOH aqueous solution). Importantly, the

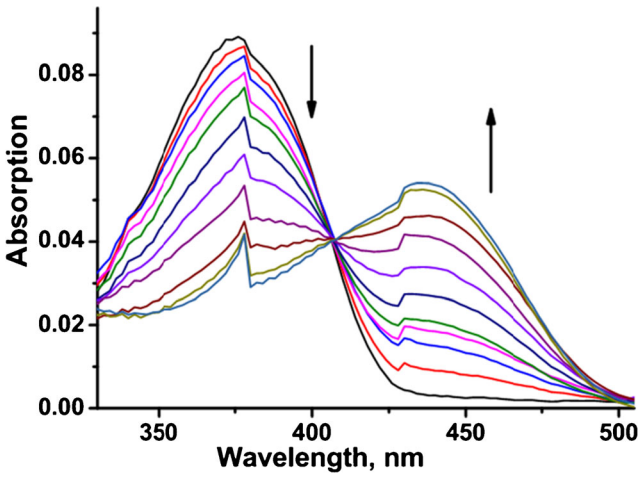

Fig. 2 Absorption spectra of probe Nap-N_3 with 0–3.5 eq. of Na_2S in 25 mM phosphate buffer (pH 7.4, containing 2 % ethanol)

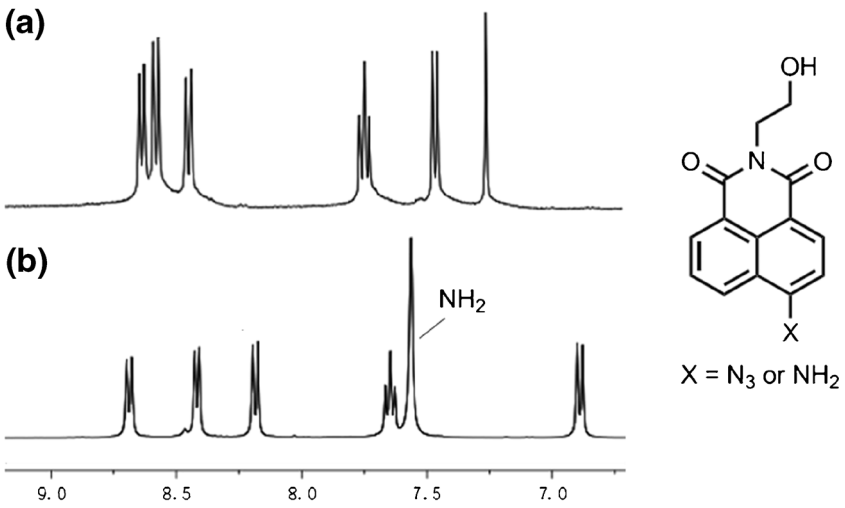

Fig. 3 The comparison of the partial ^{1}H NMR spectra of **a** Nap-N_3 in CD_3Cl and **b** Nap-NH_2 in d_6-DMSO

chemodosimeter shows an excellent linear relationship between the fluorescent emission intensities at 546 nm and the concentrations of H_2S from 0.2 to 3.0 equivalent (Fig. 1b), suggesting that the chemodosimeter is potentially useful for quantitative determination of H_2S. The ratio changes were observed in absorption spectra, as shown in Fig. 2, upon addition of H_2S, the absorption of naphthalimide azide at around 376 nm gradually faded and simultaneously a new red-shifted (62 nm) absorption band at around 438 nm (characteristic absorption of amino naphthalimide) was enhanced. There is

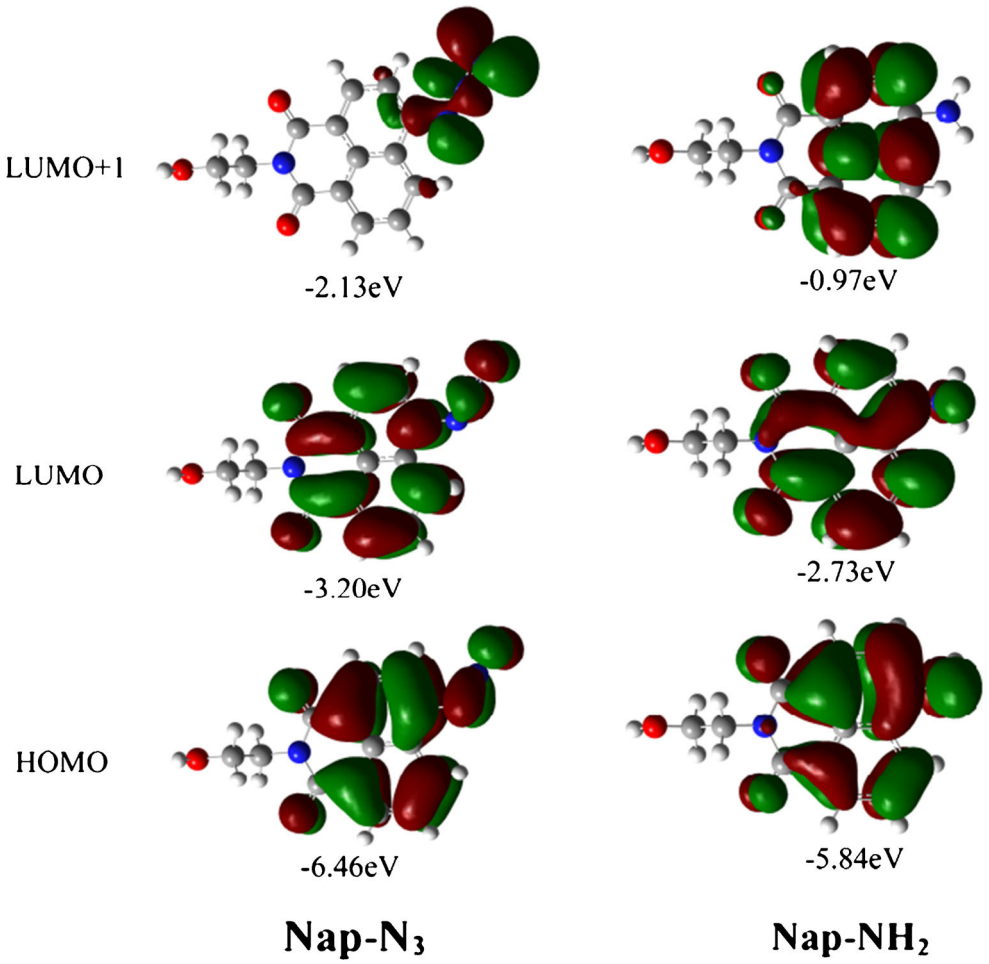

Fig. 4 Interfacial plots of the orbitals for Nap-N_3 (*left*) and Nap-NH_2 (*right*) in the excited states

a clear isosbestic point (at 407 nm) was appeared, suggesting that the conversion from **Nap-N_3** to **Nap-NH_2** is a concerted process.

Mechanism Studies

To shed light on the H_2S-triggered fluorescence turn-on response, we decided to characterize the reduced product. Incubation of **Nap-N_3** with Na_2S afforded the product, which was isolated and characterized by standard NMR and mass spectrometry (Figs. S1–3). The ^{1}HNMR spectra comparison of probe **Nap-N_3** and the product **Nap-NH_2**, the peak of NH_2 in **Nap-NH_2** was obviously observed, which suggested the resulting product should be reduced compound **Nap-NH_2** (Fig. 3). We further employed time-dependent density function (TD-DFT) to calculate the molecular orbital plots of **Nap-N_3** and **Nap-NH_2** by a suite of Gaussian 03 programs (6-31G(d) basis sets). As shown in Fig. 4, for the probe **Nap-N_3**, both the highest occupied molecular orbital (HOMO) and lowest unoccupied molecular orbital (LUMO) in the excited states are distributed on the naphthalimide backbone and azido group, however, the LUMO +1 is mainly located on the electron-withdrawing azido group. The theoretical data suggested the π electrons do not transfer from the azido unit to the naphthalimide moiety and ICT process could not occur in **Nap-N_3**. By contrast, in the case of **Nap-NH_2**, the LUMO +1 is primarily resided on the naphthalimide backbone, but not on the electron-donating amino group, which indicated the π electrons transfer to the naphthalimide moiety and ICT process occurs. These experimental facts and theoretical data supported our proposed ICT switching mechanism.

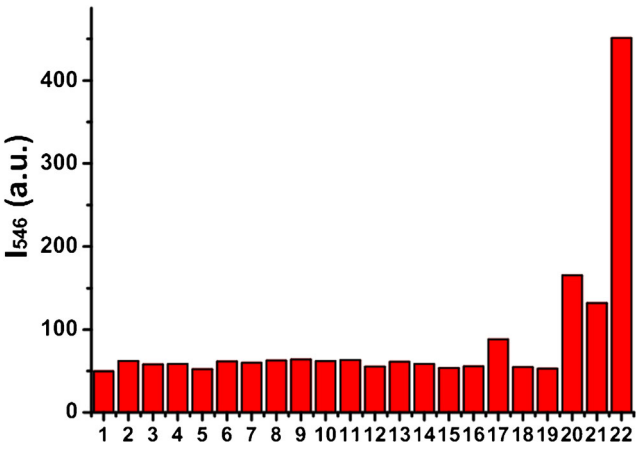

Fig. 5 Fluorescence intensity (at 546 nm) of sensor Nap-N_3 (10 μM) in the presence of various analytes in aqueous solution (pH 7.4 PBS, containing 2 % ethanol): 1, blank; 2, F^-; 3, Cl^-; 4, I^-; 5, N_3^-; 6, CO_3^{2-}; 7, SO_4^{2-}; 8, HPO_4^{2-}; 9, NO_2^-; 10, NO_3^-; 11, Ac^-; 12, SCN^-; 13, citrate; 14, $S_2SO_3^{2-}$; 15, ClO^-; 16, H_2O_2; 17, SO_3^{2-}; 18, NO; 19, ascorbic acid; 20, Cys; 21, GSH; 22, Na_2S

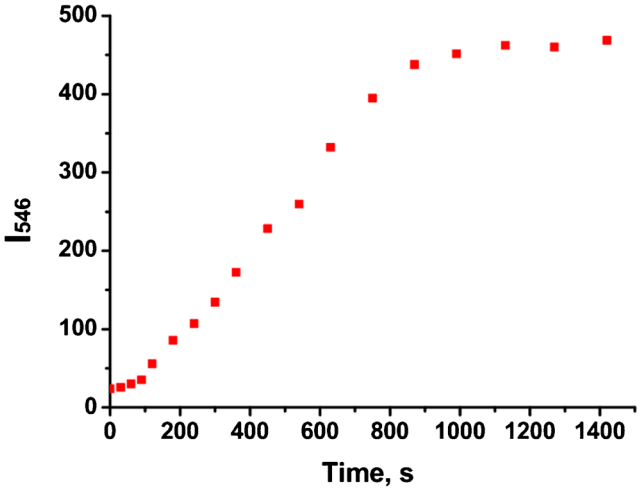

Fig. 6 Time-dependent fluorescence intensity (at 546 nm) responses of sensor Nap-N_3 (10 μM) to 3 eq.Na_2S in PBS buffer

Selectivity Studies

The detection limit was calculated to be 1.09×10^{-6} M (S/N = 3), which locates in the range of physiological concentration of H_2S in vivo, indicating that the probe is sensitive to H_2S and might be suitable for detecting endogenous H_2S in biological samples. To examine the selectivity, the probe **Nap-N_3** (10 μM) was treated with various biologically relevant species in the aqueous buffer, such as the representative anions, reactive oxygen species, reducing agents, small-molecule thiols, and Na_2S. As shown in Fig. 5, addition of the representative interfering species including F^-, Cl^-, I^-, N_3^-, CO_3^{2-}, SO_4^{2-}, HPO_4^{2-}, NO_2^-, NO_3^-, AcO^-, SCN^-, citrate at 1 mM, and $S_2O_3^{2-}$, SO_3^{2-}, ClO^-, H_2O_2, NO, ascorbic acid at 200 μM induced negligible changes. Notably, small-molecule biothiols such as glutathione (GSH) and cysteine at 1 mM triggered only a small emission intensity increase.

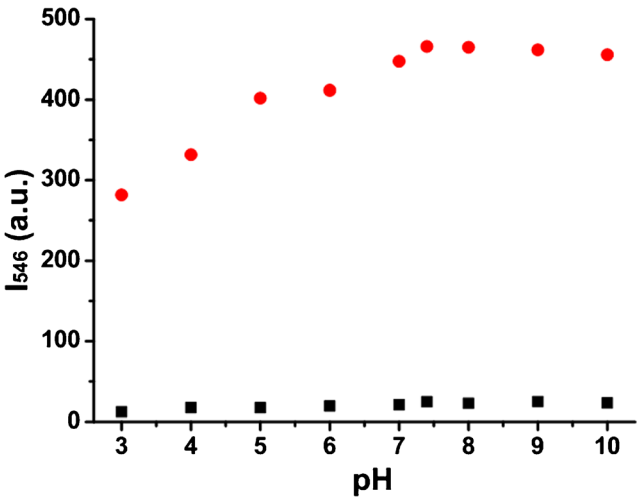

Fig. 7 The pH influence on the fluorescence intensity (at 546 nm) of Nap-N_3 (10 μM) in the absence (*black square*) or presence (*red circle*) of Na_2S (30 μM)

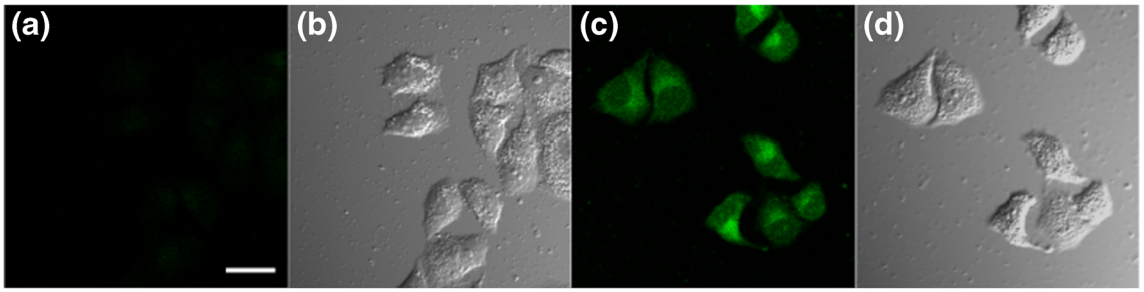

Fig. 8 Confocal fluorescence images of HeLa cells incubated with 5 μM Nap-N_3 for 20 min (**a**, **b**) and then 20 μM Na_2S for 20 min (**c**, **d**). Images (**a**, **c**) were acquired using 405 nm excitation and green emission channels of 520–570 nm; (**b**, **d**) bright field images. Scale bar = 40 μm

However, just upon addition of 30 μM Na_2S could elicit obvious increase of emission intensity.

Reaction-Time

In addition, the fluorescence intensity reached its maximum at about 15 min (Fig. 6). The results suggested the probe **Nap-N_3** has a high selectivity for H_2S over other biological species.

pH Effect

What's more, probe **Nap-N_3** could respond well to H_2S at round physiological pH (Fig. 7). The results indicated **Nap-N_3** may be suitable for studies of H_2S in the living systems.

Fluorescence Imaging in Living Cells

Firstly, to examine the cell membrane permeability of naphthalimide dye, we employed compound **Nap-NH_2** for imaging living cells. The cells incubated with **Nap-NH_2** exhibited strong fluorescence, while control cells showed none fluorescence (Fig. S4), suggesting the naphthalimide dye is cell membrane permeable. Then to examine the utility of the sensor, we intended to image H_2S in living cells. For proof-of-concept, **Nap-N_3** (5 μM) was initially incubated with HeLa cells for 20 min, after rinsed three times by PBS buffer, then treated with 20 μM Na_2S for another 20 min. As shown in Fig. 8, the cells incubated with only **Nap-N_3** exhibited faint fluorescence in the green channel. However, after co-incubation with Na_2S, strong green fluorescence was observed in living cells, suggesting **Nap-N_3** was reduced by H_2S affording fluorescent compound **Nap-NH_2**. Thus, these results revealed that **Nap-N_3** is cell membrane permeable and capable of monitoring H_2S in living cells.

In addition to detection of extraneous H_2S, we further detected the biosynthesis H_2S inside the cells. It's well-known that cystathionine β-synthase (CBS) and cystathionine γ-lyase (CSE) could catalyze cysteine for producing H_2S in living cells [28–29]. HeLa cells were firstly incubated with 200 μM cysteine for 1 h, after rinsed three times by PBS buffer, followed addition of 5 μM **Nap-N_3** and incubated another 20 min. As exhibited in Fig. 9, in comparison with the cells loaded with only the probe, the cells co-incubated with cysteine and **Nap-N_3** elicited a marked increase of fluorescence intensity in the green channel. These results further indicated that **Nap-N_3** is capable of detecting not only external H_2S in living cells, but also endogenous H_2S biologically produced by the cells.

Conclusions

In summary, we have introduced a high water-soluble H_2S fluorescent probe based on naphthalimide chromophore. The

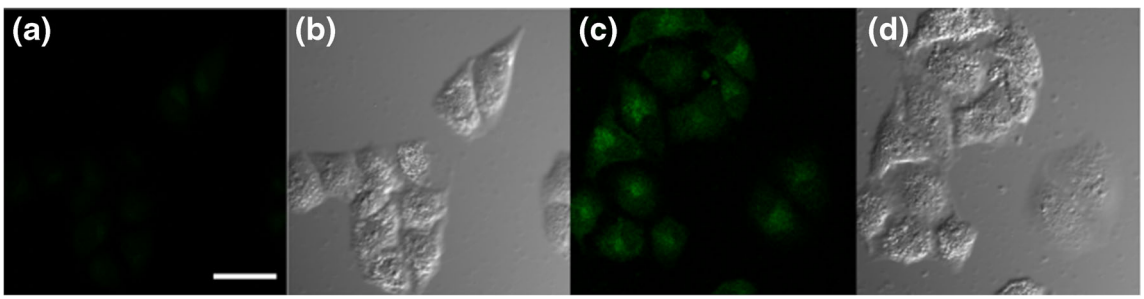

Fig. 9 Confocal fluorescence images of HeLa cells incubated with 5 μM Nap-N_3 only for 20 min (**a**, **b**) and 200 μM cystine for 1 h followed by 5 μM Nap-N_3 for 20 min (**c**, **d**). Images (**a**, **c**) were acquired using 405 nm excitation and green emission channels of 520–570 nm; (**b**, **d**) bright field images. Scale bar = 40 μm

probe **Nap-N_3** exhibits a turn-on fluorescence signal for responding H_2S via ICT switching mechanism. It has a selectivity and sensitivity for in vitro H_2S over other various biologically relevant species, and could detect both the exogenous and endogenous H_2S in living cells.

Acknowledgments This work was financially supported by the National Science Foundation of China (Nos. 21172063, 21472067) and the startup fund of University of Jinan.

References

1. Calvert JW, Jha S, Gundewar S, Elrod JW, Ramachandran A, Pattillo CB, Kevil CG, Lefer DJ (2009) Hydrogen sulfide mediates cardioprotection through Nrf2 signaling. Circ Res 105:365–374
2. Szabó C (2007) Hydrogen sulphide and its therapeutic potential. Nat Rev Drug Discov 6:917–935
3. Culotta E, Koshland Jr DE (1992) NO news is good news. Science 258:1862–1865
4. Boehning D, Snyder SH (2003) Novel neural modulators. Annu Rev Neurosci 26:105–131
5. Tanizawa K, Biochem J (2011) Production of H_2S by 3-mercaptopyruvate sulphurtransferase. J Biochem 149:357–359
6. Hughes MN, Centelles MN, Moore KP (2009) Making and working with hydrogen sulfide: the chemistry and generation of hydrogen sulfide in vitro and its measurement in vivo: a review. Free Radic Biol Med 47:1346–1353
7. Elrod JW, Calvert JW, Morrison J, Doeller JE, Kraus DW, Tao L, Jiao X, Scalia R, Kiss L, Szabo C, Kimura H, Chow CW, Lefer DJ (2007) Hydrogen sulfide attenuates myocardial ischemia-reperfusion injury by preservation of mitochondrial function. Proc Natl Acad Sci U S A 104:15560–15565
8. Yang G, Wu L, Jiang B, Yang W, Qi J, Cao K, et al. (2008) H_2S as a physiologic vasorelaxant: hypertension in mice with deletion of cystathionine gamma-lyase. Science 322:587–590
9. Yang G, Wu L, Wang R (2006) Pro-apoptotic effect of endogenous H_2S on human aorta smooth muscle cells. FASEB J 20:553–555
10. Yang W, Yang G, Jia X, Wu L, Wang R (2005) Activation of K_{ATP} channels by H_2S in rat insulin-secreting cells and the underlying mechanisms. J Physiol Lond 569:519–531
11. Peng YJ, Nanduri J, Raghuraman G, Souvannakitti D, Gadalla MM, Kumar GK, Snyder SH, Prabhakar NR (2010) H_2S mediates O_2 sensing in the carotid body. Proc Natl Acad Sci U S A 107: 10719–10724
12. Eto K, Asada T, Arima K, et al. (2002) Brain hydrogen sulfide is severely decreased in alzheimer's disease. Biochem Biophys Res Commun 293:1485–1488
13. Kamoun P, Belardinelli MC, Chabli A, et al. (2003) Endogenous hydrogen sulfide overproduction in Down's syndrome. Am J Med Genet 116A:310–311
14. Fiorucci S, Antonelli E, Mencarelli A, Orlandi S, Renga B, Rizzo G, Distrutti E, Shah V, Morelli A (2005) The third gas: H_2S regulates perfusion pressure in both the isolated and perfused normal rat liver and in ci rrhosis. Hepatology 42:539–548
15. Ueno T, Nagano T (2011) Fluorescent probes for sensing and imaging. Nat Methods 8:642–645
16. Kobayashi H, Ogawa M, Alford R, Choyke PL, Urano Y (2010) New strategies for fluorescent probe design in medical diagnostic imaging. Chem Rev 110:2620–2640
17. Li W, Sun W, Yu X, Du L, Li M (2014) Coumar in-based fluorescent probes for H_2S detection. J Fluoresc 23:181–186
18. Cai Y, Li L, Wang Z, Sun JZ, Qin A, Tang BZ (2014) Sensitivity tuneable tetraphenylethene-based fluorescent probe for directly indicating the concentration of hydrogen sulfide. Chem Commun 50: 8892–8895
19. Qiao Q, Zhao M, Lang H, Mao D, Cui J, Xu Z (2014) A turn-on fluorescent probe for imaging lysosomal hydrogen sulfide in living cells. RSC Adv 4:25790–25794
20. Ozdemir T, Sozmen F, Mamur S, et al. (2014) Fast responding and selective near-IR Bodipy dye for hydrogen sulfide sensing. Chem Commun 50:5455–5457
21. Adarsh N, Krishnan MS, Ramaiah D (2014) Sensitive naked eye detection of hydrogen sulfide and nitric oxide by aza-BODIPY dyes in aqueous medium. Anal Chem 86:9335–9342
22. Sun W, Fan J, Hu C, Cao J, Zhang H, Xiong X, Wang J, Cui S, Sun S, Peng X (2013) A two-photon fluorescent dye with near-infrared emission for hydrogen sulfide imaging in biosystems. Chem Commun 49:3890–3892
23. Wan Q, Song Y, Li Z, Gao X, Ma H (2013) In vivo monitoring of hydrogen sulfide using a cresyl violet-based ratiometric fluorescence probe. Chem Commun 49:502–504
24. Wang K, Peng H, Ni N, Dai C, Wang B (2014) 2,6-dansyl azide as a fluorescent probe for hydrogen sulfide. J Fluoresc 24:1–5
25. Liu XL, Du XJ, Dai CG, et al. (2014) Ratiometric two-photon fluorescent probes for mitochondrial hydrogen sulfide in living cells. J Org Chem 79:9481–9489
26. Yu C, Li X, Zeng F, Zheng F, Wu S (2013) Carbon-dot-based ratiometric fluorescent sensor for detecting hydrogen sulfide in aqueous media and inside live cells. Chem Commun 49:403–405
27. Lakowicz JR (1999) Principles of fluorescence spectroscopy, 2nd edn. Kluwer Academic/Plenum Publishers, New York
28. Qian Y, Karpus J, Kabil O, Zhang SY, Zhu HL, Banerjee R, Zhao J, He C (2011) Selective fluorescent probes for live-cell monitoring of sulphide. Nat Commun 2:495–501
29. Yang S, Qi Y, Liu C, Wang Y, Zhao Y, Wang L, Li J, Tan W, Yang R (2014) Design of a simultaneous target and location-activatable fluorescent probe for visualizing hydrogen sulfide in lysosomes. Anal Chem 86:7508–7515